NANO LETTERS

2001
Vol. 1, No. 1
36−41

Theoretical Studies of Electronic State Localization and Wormholes in Silicon Quantum Dot Arrays

Barton B. Smith* and A. J. Nozik

National Renewable Energy Laboratory, 1617 Cole Blvd., Golden, Colorado 80401

Received October 6, 2000

ABSTRACT

We present calculations for quantum dot (QD) arrays that are more realistic than most. They describe the arrays in atomic detail, using pseudopotentials fit to ab initio results to describe the electronic structure. Our results show that simple models, which regard QDs as (artificial) atoms, are a reasonable approximation to employ for some features of QD array electronic localization characteristics. But we also demonstrate important limitations. The need for realistic theoretical descriptions of QD arrays is highlighted.

1. Introduction. Collections of essentially isolated quantum dots (QDs) have been extensively studied theoretically and experimentally. Prodigious effort has also been devoted to electronically interacting QDs in arrays because of important applications, especially those which involve QD array superlattices.[1−4] But understanding of electronically coupled QD arrays lags behind isolated systems. The former systems are the subject of this letter, and we will focus on the issue of localization of electronic states in them.

Many kinds of electronically coupled QD array systems have been examined experimentally,[1,2,5−7] and the electronic state localization in these systems has been examined.[2,5,7−9] Localization phenomena remain controversial for many of these systems.

A large number of theoretical studies on QD arrays in the solid-state literature use the simple Anderson−Newns or Hubbard-type model Hamiltonians.[10−13] Each QD is regarded as an atom in the majority of these studies, in accord with the often well-justified approximation of viewing QDs as artificial atoms. However, it is not self-evident that such an approach will accurately describe real QD array systems. Our calculations, which treat QD arrays in atomic detail, indicate the electronic coupling between the QDs in the array can be a sensitive function of their configuration and surface structure. Artificial atom QD approaches cannot probe these effects- the interdot coupling is simply parametrized. We find the QD array wave functions themselves can be very complicated and difficult to map onto simple atomic-like basis sets. There is a pronounced dearth of higher level calculations that treat QD arrays realistically, i.e., in atomic detail. Thus, especially in light of the other points above, realistic studies of QD arrays seem fully warranted.

It is appropriate to briefly review electronic state localization phenomenon in the context of QD array systems. Electronic states can become localized even in crystalline bulk solids by various kinds of deviations from perfect crystal structure (introduced impurities, dislocations, adsorbed species, surfaces, etc.). In typical noncrystalline materials, where the atomic structure is amorphous, the disorder can be so great that all or nearly all of the electronic states in the system become localized to some degree.[14,15] In these systems, states are often spatially localized near one or a small number of atoms. However, with our QD array systems, we will be primarily concerned with states that are localized on one or a few QDs (not atoms). There are a number of ways that this can occur. The QD size can vary and cause disorder in the array superlattice, which changes both the band offset between dots and their electronic coupling. The surface structure of the dots can vary, which dramatically affects the coupling, and also can cause charge transfer between the dots which changes the atomic energetics. The QDs can also be at random orientations and distances relative to each other, and this can cause significant differences in the electronic coupling between dots.

If all electronic states were localized in a system, and therefore, no extended state channels remained, the principal means of conduction would be through phonon assisted hopping.[14,16] In less disordered systems, both localized and extended state conduction is possible. Thus, to characterize carrier transport properties in QD array systems, it is crucially important to ascertain the extent of localization, just as it is in noncrystalline materials,[14−16] and we devote our attention to this below. Perfectly ordered arrays of identical QDs are an idealization, and may remain so far into the future.

We focus our studies primarily on systems that have no material between the dots, i.e., the matrix in which they are embedded is vacuum. This allows examination of the effects of QD disorder itself uncomplicated by matrixes. We keep

10.1021/nl0001858 CCC: $20.00
Published on Web 12/19/2000

the separation between QDs small enough that the electronic coupling is high and Coulomb blockades and related effects can be expected to be attenuated.[17,18] We do not consider electron−electron interactions as an agent of localization.[17] We also do not address phonon localization here, nor do we directly address phonon involvement in transport, although we have done this elsewhere.[19,20] Nonetheless, because our studies allow the characteristics of $T = 0$ localization to be established, the character and degree of phonon assisted transport for $T \neq 0$ can be ascertained, as it is in other systems.[14,15]

2. Methodology. We employ a number of approaches for these very computationally demanding systems. We use ab initio calculations, including B3LYP density functional theory (DFT), as well as standard quantum chemistry basis sets implemented via Gaussian 98 and Jaguar v3.0,[21,22] on small QD arrays consisting of just two QDs, and also to scrutinize the electronic structure of single dots. These results serve as checks on lower level calculations and are used to parametrize them (vide infra). For studies of large arrays in this letter, we focus on results from a pseudopotential method that is a non-self-consistent field approach, which is described in the next paragraph. As an additional check on this method, we employ one of the few tractable self-consistent field (SCF) approaches for very large systems. This is a semi-empirical approach from quantum chemistry—the PM3 Hamiltonian of MOPAC.[23]

We now begin to describe the pseudopotential method employed here for large QD arrays. The empirical pseudopotential method (EPM) has a long history in solid-state physics.[24] It remains one of the few methods used for addressing a number of excited-state properties in solid-state systems. It uses a linear superposition of atomic pseudopotentials V_{atomic} ($\mathbf{r}$) to represent the total system potential

$$V_{\text{total}}(\mathbf{r}) = \Sigma_i V_{\text{atomic}}(\mathbf{r}-\mathbf{r_i}) \qquad (1)$$

where $\mathbf{r_i}$ is the atomic real space vector. The time independent Schrödinger equation is then solved using this $V_{\text{total}}(\mathbf{r})$. In the EPM, $V_{\text{total}}(\mathbf{r})$ is Fourier transformed to reciprocal space and a plane wave basis set used. The weakness of this method is of course that, like standard tight binding methods, it is not a self-consistent field methodology.

Our overall approach is very similar to EPM and closer still to an LCAO approach, which has found great success for bulk solid-state properties.[25] In our method, we employ eq 1 in its real space form. We start with standard local EPM pseudopotentials[24] in real space; these are essentially identical to those detailed in ref 25. But we find the surface atomic pseudopotentials need to be different than bulk, to some extent, to best match our one dot B3LYP DFT ab initio studies, and we adjust these (for H and outer Si atoms). To solve the time independent Schrödinger equation for the system, we use the same LCAO s,p,d, minimal real space basis set expanded in GTOs as ref 25. (Both real and reciprocal space basis sets have well-known advantages and disadvantages for systems of the general kind examined here).[26] Our method is thus a hybrid of EPM and LCAO, and we call it the augmented (augmented by changing surface atom pseudopotentials) real space empirical pseudopotential (ARSEP) method. We find, via ab initio B3LYP DFT and HF SCF calculations, that the small pseudopotential corrections mentioned are also sufficient when the dots are electronically interacting, as long as they are far enough apart, in part because the charge exchange is small and because the dipole moment is very small (our ab initio results show it is of order 0.001 D for the 10 Å QDs used below). Thus, this nonself-consistent field approach is at least partially justified. We have described other details of this general method elsewhere.[19]

There are a number of measures of electronic state localization,[14] but we will use essentially one below. This method simply involves summing the probability density on each dot for each state. We then calculate for each state how many dots contain 98% (or other percentages) of the total probability density for that state. We will call this measure the dots per state (DPS). Obviously, this method is closely related qualitatively to the well-known participation ratio localization measure.[14] There is some ambiguity in the DPS measure, and the problems are analogous to the well-known ones of Mulliken charge analysis.[27] But in practice, because we deal with probability density on large entities (QDs), rather than atoms, the problems are decreased.

The well-known standard definitions of extended and localized states[14,15] can be problematic when small devices are considered, as we now illustrate. For example, assume a characteristic localization length for some states in a large system is of 100 Å scale. If we cut out a chunk of this system of scale 100 Å some groups of states, which are localized by standard definitions, may be quasi-extended. That is, in this sized system, these states will have significant probability density throughout the system and an electron wave packet placed in such states will propagate through the system. Thus, the system will conduct (from one end of the device to the other) through such a state at $T = 0$. This is the main feature of interest in many small devices, and the localized state then is, for all practical purposes, extended. Already in the literature such states in small devices are called, simply, extended states. But to avoid confusion below, we will call all states that span the device under consideration "quasi-extended" states, unless we can prove they are extended in the standard sense.

3. Results and Discussion. The arrays we focus on in this Letter use a QD cut from bulk Si, and we passivate the surface Si atoms (which are not fully coordinated) with hydrogen atoms set at configurations optimized via ab initio calculations (LACVP basis set),[21] while holding the Si framework fixed (the H−Si bond length on average is a little less than 1.5 Å). This QD is as spherically shaped as possible for its size of about 10 Å in diameter (D). We will call this dot the $D = 10$ Å QD (it has 29 Si atoms). The set A eigenvalues in Figure 1 are results from a ARSEP calculation on this QD, and these eigenvalues (and eigenstates) match ab initio calculations (B3LYP DFT) that we have performed on this dot well. The zero of energy in Figure 1 was set at

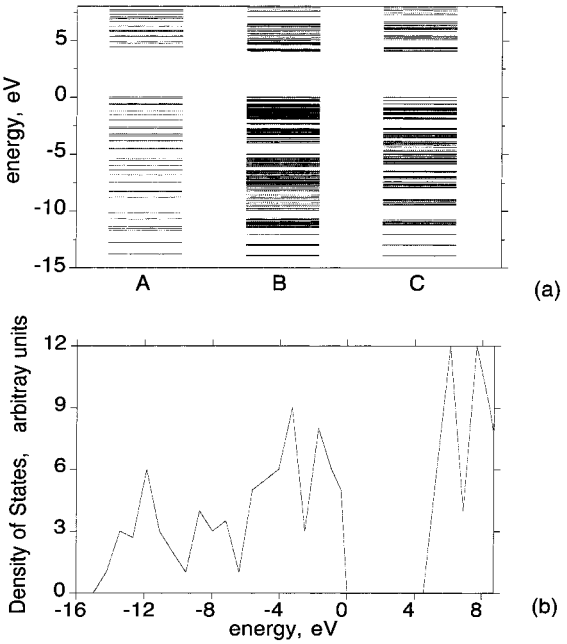

Figure 1. Plots of the eigenvalues for (A) The isolated $D = 10$ Å QD and (B) The ordered 1D QD array of twelve QDs. (C) A representative 1D QD array from the 20 disordered 1D QD arrays composed of twelve QDs.

the $D = 10$ Å QD HOMO eigenvalue. Figure 1, set A, shows that the eigenvalues of the $D = 10$ Å QD appear rather discrete on the energy scale used. But when we bin these eigenvalues to form Figure 1b, one sees that the density of states is already similar to bulk Si. The width of the valence band is somewhat larger than bulk, in accord with our ab initio calculations.

As can be seen in set A of Figure 1, the ARSEP calculation gives a value of about 4.4 eV for the main band gap of the $D = 10$ Å QD, and this is in accord with previous calculations uncorrected for Coulomb interactions.[28−31] These standard corrections have undergone recent scrutiny and remain somewhat controversial.[29−31] Thus, it seems appropriate to report uncorrected data. Experiments indicate band gaps for Si QDs are actually smaller than predicted by theory, even with Coulomb correction.[32] But controversy surrounds these matters as well. The absolute size of the band gap is rather unimportant for our studies below since we focus on one size of QD (we do not explore band gap vs QD size). Band gaps, of course, remain difficult to predict accurately theoretically, even for the highest level methods, for well-known reasons.[24,26]

We will focus on smaller QDs and arrays for a number of reasons. Perhaps the majority of previous theoretical studies use very small arrays, many consider only two QDs, so our results can be easily compared to these. Smaller arrays allow us to use PM3 SCF calculations to probe charge redistribution. We are interested in strongly electronically coupled QD arrays, and we have calculated that the electronic coupling can be quite significant with the $D = 10$ Å dots (vide infra). Many devices propose to make use of very small arrays. Finally, smaller dots and arrays save computational resources. We will briefly discuss our studies of larger QDs and arrays

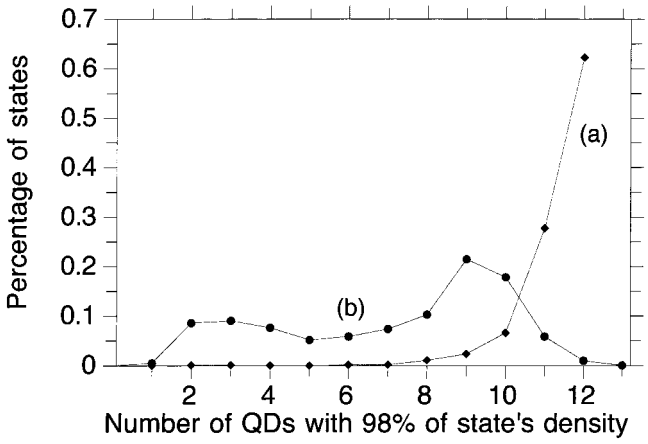

Figure 2. Plots of the dots per state (DPS) needed to account for greater than 98% of the probability density in a given state for (a) the ordered 1D twelve QD array (b) the average DPS for the ensemble of 20 disordered 1D twelve QD arrays.

below which show little loss of generality is involved in using smaller ones.

When QD arrays are composed of far separated $D = 10$ Å QDs, the eigenvalues of the entire system look, of course, just like set A of Figure 1. If the QDs are spaced close to each other, and their electronic coupling thus becomes significant, these rather discrete states begin to form subbands. Let us explore aspects of this by first taking the $D = 10$ Å QDs and aligning them linearly, by translating them in the (001) direction of the QD, with their crystal directions thus all pointing in the same Cartesian direction and with their passivating endmost hydrogens consequently at right angles relative to each other. We space the dots equidistantly from each other and use a total of twelve dots. The closest hydrogens in this 1D array were 1.3 Å from each other, and these comprised only about four per dot. The eigenvalues for the ordered array we just described are set B of Figure 1. The subbands, which are seen to be formed in set B of Figure 1, are analogous to those that form in quantum well superlattices, thus they can be called minibands. Curve (a) of Figure 2 plots the DPS (dots per state, see method section) for this ordered system for states near the top/bottom of the main valence band (VB)/conduction band (CB) energy region of the $D = 10$ Å QD (we used states 4 eV into the $D = 10$ Å QD VB and CB; compare eigenvalues of set A with set B in Figure 1 to identify these regions). These states are of most interest for transport properties in many proposed devices. Note that the states in curve (a) of Figure 2 are significantly delocalized over the small system we use, indeed this figure shows almost all the QDs in the system are needed to account for 98% of the probability density in each state shown. Many of the states in this ordered QD array are highly degenerate, and we of course use appropriate wave function superpositions to calculate the DPS. Most states in this system are extended in the standard sense of the term.

Let us begin a study of localization for 1D arrays by using the same array of twelve QDs discussed immediately above, except we now move the QDs randomly in 1D (along the axis which runs through the dot centers). We keep the

random separation distance between the QDs small enough that the electronic coupling between all dots remains high (we quantify this coupling as the standard electronic coupling matrix element for electron transfer,[33] and we calculate that for nearest neighbor dots, this was kept greater than order 0.01 eV). The hydrogen to hydrogen distances between dots were constrained between a minimum of 1.2 Å, and a maximum of 1.6 Å. The set C eigenvalues of Figure 1 are from one random configuration with these constraints (we used a total of 20 random configurations) and this figure shows that minibands again form. However, in these more realistic (disordered) QD arrays the character of the electronic states is different than usually considered in quantum well superlattices. One of the most significant differences is that these array minibands contain a substantial number of localized states. Curve (b) of Figure 2 plots the average dots per state for 20 configurations, using the constraints described, for states in the top/bottom 4 eV of the main VB/CB, respectively. It can be clearly seen, in comparison with curve (a) of Figure 2 (which is for the ordered 1D array), that many of the states are localized. However, some of the states have significant probability density on each dot (see curve (b) of Figure 2), and are thus quasi-extended states (theory predicts that in a true 1D system with any disorder all states are localized; obviously, our system is atomically 3D).[14] In passing, we note that greater separation distances between the dots, of course, decreases the electronic coupling. We find mixing and minibands occur even at a H−H distance (between QDs) of 2.4 Å (our current largest separation distance). PM3 geometry optimization shows our closest separation distances are physically realizable in a vacuum matrix, but the matrix can prohibit this close separation in real systems.

Let us now look at higher dimensional array configurations. We have done many studies of two and three-dimensional Si QD arrays. We will focus on one of the three-dimensional ones. This study used twelve of the $D = 10$ Å QDs above in the following configuration. A perfectly ordered 3D array was constructed by placing four QDs at corners of a square and using three layers of these squares. All crystal faces of the QDs pointed in the same direction (same as above). The endmost hydrogens (those parallel to the long axis) were again at right angles to each other. Figure 3, set A, plots the eigenvalues for this system, and shows the minibands which result from the ARSEP calculation on this 3D QD array. Figure 4 shows the dots per state for states near the top/bottom 4 eV of the main VB/CB, respectively. Figure 4, curve (a), shows that in this perfectly ordered 3D "crystal" these states are highly delocalized, and many of these are highly degenerate. Standard extended states exist.

We constructed another 3D QD array the same way as in the last paragraph, except we altered the array so that it was significantly disordered. We did this by moving each dot's center randomly from those of the last paragraph, and we also randomly rotated the dots about their spatial center. As in the 1D case, the hydrogen to hydrogen distances between dots were constrained to lie between a minimum of 1.2 Å, and a maximum of 1.6 Å. The eigenvalues for this system

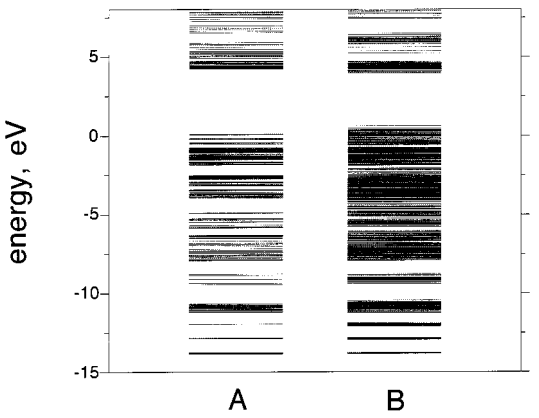

Figure 3. Plots of the eigenvalues for (A) The ordered 3D QD array of twelve QDs. (B) A representative 3D QD array from the 20 disordered arrays composed of twelve QDs. Same energy scale as Figure 1.

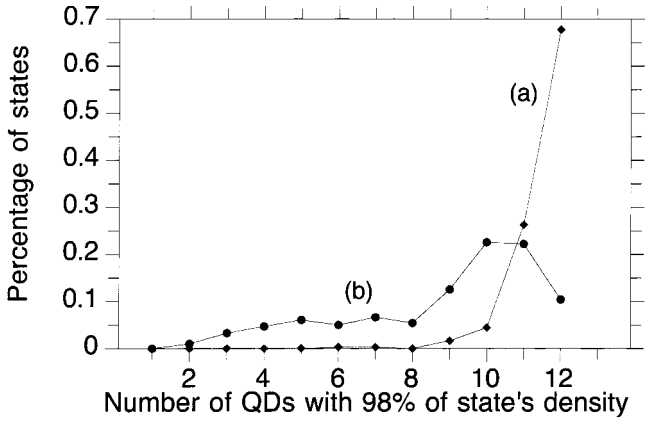

Figure 4. Same as Figure 2 except this plots the dots per state (same 98% criterion) for (a) the ordered 3D QD array of twelve QDs (b) the average DPS for the 20 strongly disordered 3D QD arrays.

are shown in set B of Figure 3, as calculated via ARSEP, and minibands are again seen. Figure 4, curve (b), shows the dots per state 4 ev into the CB and VB. Comparison of curve (a) and (b) in Figure 4 show some obvious localization in the 3D disordered system. However when Figure 4 is compared to Figure 2 one sees the localization in this strongly disordered 3D system is less than for the disordered 1D array (curve (c) Figure 2). We find the latter is general for these systems regardless of what measure of localization is used. Thus, our calculations agree with standard ideas regarding disordered (atomic) systems, which show that it is harder to induce localization in higher dimensional systems (2D and 3D) than 1D systems.[14,16,34,35] We note our calculations show that the states on the edges of the subbands tend to be localized, and that states nearer the middle of the subbands are more extended, also in agreement with the standard notions about disordered atomic systems.[14] This tendency is also displayed in the 1D arrays to varying degrees.

We have made extensive studies of other 1D, 2D, and 3D arrays of dots. We have not made a full systematic analysis of these results, and additional calculations remain, but trends have already emerged. Localization can be quite pronounced when we use different sized dots (as are present in

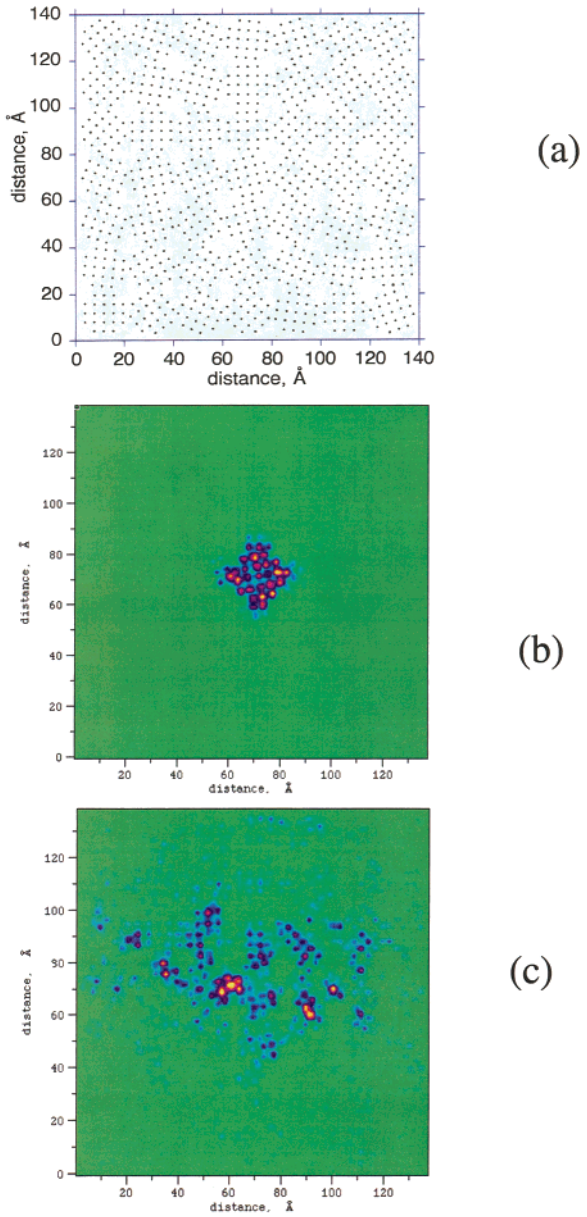

Figure 5. (a) Cross section through the 2D QD array described in the text, which shows the position of the Si atoms in the middle of a QD array composed of spherical Si dots of about 18 Å in diameter. (b) The same cross section showing the probability density early in the simulated photoexcitation when it is near the middle QD in which the excitation is initialized (the spreading of probability density into adjacent dots can be seen). (c) The same cross section showing the probability density later in time when the electron wave packet has propagated into the space allowed by the state described in the text. Regions colored yellow have the highest probability density followed by orange,red, violet, blue, and green.

experimental systems)[36] and/or oxidized and reconstructed surfaces. Experiments already show that both localized and extended (at least quasi-extended) states play a role in transport (see introduction references), and this agrees qualitatively with our theoretical investigations. That is, we find, so far, that as long as the dots themselves are primarily crystalline (as opposed to amorphous) that even our most disordered systems do have some states that extend at least on the order of 100 Å near the main gap that can allow $T = 0$ conduction (electron/hole transport) through a small array of dots. We are in the process of comparing experiments[2,5,7,9] to quantitative predictions of our calculations regarding energetics (where localized and extended states lie in energy) and conductivity.

We have assumed in this paper that the matrix in which the QDs are embedded is vacuum. But in many QD array systems organic molecules form the matrix. We have done calculations with simple hydrocarbons as a matrix between very small arrays, and the matrix can significantly affect localization. Some organics can electronically couple strongly with the QDs. It may prove possible to find superexchange molecular bridges between dots which will allow high coupling between dots and improve transport through the system significantly.

We have performed tight binding as well as ARSEP calculations with larger ($D = 20$ Å dots) in QD arrays larger than 40 dots and found conclusions in qualitative agreement with those above. In these larger array systems, it is possible to pack the dots in hexagonal and other geometries that experimental images show occur in many QD array systems.

We now take the same pseudopotentials used in our ARSEP method and solve not the time independent, but the time dependent Schrödinger equation (via techniques discussed elsewhere)[19] for electron wave packets in these QD arrays.

In Figure 5, we show the results of a calculation for simulated photoexitation (promotion of an electron from the VB to the CB) of an electron (wave packet) in the middle QD (see Figure 5a) in the two-dimensional QD array shown in the figure. The picture of the electron probability density (as a function of time) in the figure is a slice through the middle of the array of $D = 18$ Å QDs; 49 dots were used. All the QDs are randomly rotated relative to each other only in the plane of Figure 5; they have the same orientation in a perpendicular plane. Note the wave packet propagates throughout the array in the direction of the horizontal axis. Spreading of the wave packet is essentially prohibited (by the disorder) in this state in the vertical direction of Figure 5. Thus the state is quasi-extended, in effect, only in the horizontal direction. Because the state shown is a quasi-extended state, it does not require phonon participation to propagate from one (horizontal) end of the array to the other (we use $T = 0$ here). If leads were on the left and right side of the array, and an electric field applied (which did not significantly distort the state), a significant current could be measured. Thus, the state is a diffuse wormhole for transport oriented in primarily one direction. We have also done these calculations for 3D arrays, which also show wormholes; the graphics is most easily rendered for 2D arrays. We have performed many of these time dependent wave packet propagation calculations and we find that wormholes, of an often very circuitous nature, exist even in very disordered large QD array systems (more than 60 QDs). We have also looked at the role of phonons and applied fields in these systems regarding localization; these complex effects will be reported elsewhere.

4. Conclusion. We have presented calculations above for QD arrays that are more realistic than most. Our results

demonstrate that, as in other areas of QD phenomena, simple models which regard QDs as "atoms" are a reasonable approximation for some features of QD behavior. Indeed our results showed localization phenomena have some similar characteristics in QD arrays and atomic systems. But we also demonstrated that key features are not addressed. In short, it is essentially impossible for "artificial atom" approaches to predict what effects surface structure, crystal face orientation, reconstructions, etc. have on the amount of disorder and where (in energy and space) the resultant states will be localized in QD arrays because the "artificial atom" approaches can only parametrize these effects. Thus, it appears that the artificial atom outlook has important limitations for QD arrays, and that there is a marked need for extensive realistic higher level studies.

We saw that even in QD arrays composed of identical QDs localization appears. Real world dots can be expected to have a greater degree of localization, as the preliminary calculations we reported showed. We have performed apparently the first calculations of wave packet propagation through realistic array systems, and found that quasi-extended state wormholes can exist even in very disordered systems. Our calculations predict mixed extended and localized state conduction through disordered real world self-assembled small QD systems can occur, in accord with existing experiments (vide supra) on small systems. This has important implications for numerous QD array devices, especially for devices that must have coherence to function. Theoretical studies such as the present can serve to elucidate how localization influences various real world systems, and help lead the way to practical QD devices.

Acknowledgment. This work was supported by the U.S. Department of Energy, Office of Basic Energy Sciences, Office of Energy Research, Division of Chemical Sciences.

References

(1) Gaponenko, S. V. *Optical Properties of Semiconductor Nanocrystals*; Cambridge University Press: New York, 1998.
(2) Lan, S.; Akahane, K.; Jang, K.-Y.; Kawamura, T.; Okada, Y.; Kawabe, M.; Nishimura, T.; Wada, O. *Jpn. J. Appl. Phys.* **1999**, *38*, 2934.
(3) Stangl, J.; et al. *J. Vac. Sci. Technol., B* **2000**, *18*, 2187.
(4) Springholz., G.; Holy, V.; Pinczolits., M.; Bauer, G. *Science* **1998**, *282*, 734.
(5) Schedelbeck, G.; Wegscheider, W.; Bichler, M.; Abstreiter, G. *Science* **1997**, *278*, 1792.
(6) Solomon, G. S.; Trezza, J. A.; Marshall, A. F.; Harris, J. S. **1996**, *76*, 952.
(7) Lan, S.; Akahane, K.; Song, H.-Z.; Okada, Y.; Kawabe, M. *Phys. Rev. B.* **2000**, *61*, 16 847.
(8) Artemyev, M. V.; Bibik, A. I.; Gurinovich, L. I.; Gaponenko, S. V.; Woggon, U. I. *Phys. Rev. B.* **1999**, *60*, 1504.
(9) Oosterkamp, T. H.; Fujisawa, T.; Wiel, W. G.; Ishibashi, K.; Hijman, R. V.; Tarucha, S.; Kouwenhoven, L. P. *Nature* **1998**, *395*, 873.
(10) Kotlya, R.; Stafford, C.; Sarma, S. *Phys. Rev. B.* **1998**, *58*, 3989.
(11) Guanlong, C.; Klimeck, G.; Datta, S.; Goddard, W. A. *Phys. Rev. B* **1994**, *50*, 8035.
(12) Anderson, P. W. *Phys. Rev.* **1961**, *124*, 41.
(13) Newns, D. M. *Phys. Rev.* **1969**, *178*, 1123.
(14) Elliott, S. R. *Physics of Amorphous Materials*; Longman: London, 1984.
(15) Adler, D.; Schwartz, B.; Steele, M. *Physical Properties of Amorphous Materials*; Plenum: New York, 1985.
(16) Mott, N. *Conduction in Non-Crystalline Materials*; Oxford Clarendon Press: Oxford, 1987.
(17) Lin, L. H.; Aoki, N.; Nakao, K. *Phys. Rev. B.* **1999**, *60*, R16 299.
(18) Kirczenow, G. *Phys. Rev. B.* **1992**, *46*, 1439.
(19) Smith, B. B.; Nozik, A. J. *J. Phys. Chem. B.* **1999**, *103*, 9915.
(20) Smith, B. B.; Nozik, A. J. *J. Phys. Chem. B* **1997**, *101*, 2459.
(21) *Jaguar v3.0 Schrödinger* Portland, OR, 1997.
(22) Frisch, M. J.; Trucks, G. W.; Schlegel, H. B.; Scuseria, G. E.; Robb, M. A.; Cheeseman, J. R.; Zakrzewski, V. G.; Montgomery, J. A.; Stratmann, R. E.; Burant, J. C.; Dapprich, S.; Millam, J. M.; Daniels, A. D.; Kudin, K. N.; Strain, M. C.; Farkas, O.; Tomasi, J.; Barone, V.; Cossi, M.; Cammi, R.; Mennucci, B.; Pomelli, C.; Adamo, C.; Clifford, S.; Ochterski, J.; Petersson, G. A.; Ayala, P. Y.; Cu, Q.; Morokuma, K.; Pople, J. A. *Gaussian 98 (Revision A.7)*; Pittsburgh, PA, 1998.
(23) Stewart, J. J. P. *MOPAC 93.00 Manual*; Fujitsu Ltd.: Tokyo, Japan, 1993.
(24) Cohen, M. L.; Chelikowsky, J. R. *Electronic Structure and Optical Porperties of Semiconductors*; Springer-Verlag: New York, 1988; Vol. 75.
(25) Huang, M.; Ching, W. Y. *J. Phys. Chem. Solids* **1985**, *46*, 977.
(26) Ellis, D. E. *Density Functional Theory of Molecules, Clusters, and Solids*; Kluwer Academic Pub.: Boston, 1995.
(27) Levine, I. N. *Quantum Chemistry*; Simon and Schuster: New Jersey, 1991.
(28) Wang, L.; Zunger, A. *J. Phys. Chem.* **1994**, *98*, 2158.
(29) Franceschetti, A.; Wang, L.; Zunger, A. *Phys. Rev. Lett.* **1999**, *83*, 1269.
(30) Ogut, S.; Chelikowsky, J. R.; Louie, S. G. *Phys. Rev. Lett.* **1997**, *79*, 1770.
(31) Godby, R. W.; White, I. D. *Phys. Rev. Lett.* **1998**, *80*, 3161.
(32) Buuren, T. v.; Dinh, L. N.; Chase, L. L.; Siekhaus, W. J.; Terminello, L. J. *Phys. Rev. Lett.* **1998**, *80*, 3803.
(33) Farazdel, A.; Dupuis, M.; Clementi, E.; Aviram, A. *J. Am. Chem. Soc.* **1990**, *112*, 4206.
(34) Abrahams, E.; Anderson, P. W.; Licciardello, D.; Ramakrishnan, T. **1979**, *42*, 673.
(35) Mott, N. F. *Philos. Mag.* **1981**, *B44*, 265.
(36) Micic, O. I.; Jones, K. M.; Cahill, A.; Nozik, A. J. *J. Phys. Chem. B* **1998**, *102*, 9791.

NL0001858